UNSTEADY NATURAL CONVECTION HEAT TRANSFER IN A DOMAIN PARTLY FILLED WITH POROUS SUBSTRATE USING THE BRINKMAN-EXTENDED DARCY MODEL.

Dr. A. F. KHADRAWI
Mechanical Engineering, Al-Balqa' Applied University
Al-Salt, Jordan

The problem of transient free convection in a domain partly filled with porous substrate is investigated using the Laplace transformation technique. A porous substrate attached to one of the heated walls is considered. The Brinkman-extended Darcy model is adopted to describe the hydrodynamics behavior of the porous domain. The effect of some parameters, such as thermal conductivity ratios and thermal diffusivity ratios, on the temperature and velocity distributions is investigated.

Introduction

The use of porous substrates to improve convective heat transfer in channels has many practical, geophysical, environmental, and technological applications. Examples include electronic cooling, chemical and nuclear reactors, heat transfer from hair covered skin, porous flat plate collectors, grain and food storage and drying, solidification of concentrated alloys, packed bed thermal storage, and fibrous and granular insulation where the insulation occupies only part of the space separating the heated and cooled walls. The present work considers the transient free convection fluid flow problem in a domain partially filled with porous substrates.

Mathematical formulation

Consider an unsteady laminar fully developed free convection flow in a domain partly filled with porous material. The fluid is assumed to be Newtonian with uniform properties and the porous medium is isotropic and homogeneous. Also, it is assumed that both viscous dissipation and internal heat generation are absent. Using dimensionless parameters, the equations of motion and energy in both clear and porous domains are given as, respectively,

$$\frac{\partial U_1}{\partial \tau} = \frac{\partial^2 U_1}{\partial Y^2} + \theta_1, \qquad \frac{\partial \theta_1}{\partial \tau} = \frac{1}{\Pr}\frac{\partial^2 \theta_1}{\partial Y^2} \tag{1}$$

$$C_a \frac{\partial U_2}{\partial \tau} = \mu_R \frac{\partial^2 U_2}{\partial Y^2} - \frac{1}{Da} U_2 + \theta_2 \quad , \qquad \frac{\partial \theta_2}{\partial \tau} = \frac{\alpha_R}{\Pr}\frac{\partial^2 \theta_2}{\partial Y^2} \tag{2}$$

with the following initial and boundary conditions:

$$\begin{aligned} &U_1(0,Y) = U_2(0,Y) = 0.0, \qquad \theta_1(0,Y) = \theta_2(0,Y) = 0.0 \\ &U_1(\tau,0) = 0.0 \ , \qquad \theta_1(\tau,0) = 1.0 \ , \quad U_2(\tau,1) = 0.0 \quad , \quad \theta_2(\tau,1) = 1.0 \\ &U_1(\tau, r) = U_2(\tau, r), \qquad \theta_1(\tau, r) = \theta_2(\tau, r) \\ &\frac{\partial U_1}{\partial Y}(\tau,r) = \mu_R \frac{\partial U_2}{\partial Y}(\tau,r), \qquad \frac{\partial \theta_1}{\partial Y}(\tau,r) = K_R \frac{\partial \theta_2}{\partial Y}(\tau,r) \end{aligned} \tag{3}$$

where the subscript 1 and 2 refer to the clear and porous domains respectively. In Eq. (2), C_a is an acceleration coefficient tensor, and it depends on the geometry of the porous medium. The other parameters appearing in Eqs. (1-3) are defined as follows:

$$\mu_R = \frac{\mu_2}{\mu_1}, \quad K_R = \frac{k_2}{k_1}, \quad Da = \frac{K}{L_2^{\,2}}, \quad \Pr = \frac{\nu_1}{\alpha_1}, \quad r = \frac{L_2}{L_1},$$

Equations (1-2) are solved using Laplace transformation technique. Now with the notation that $L\{U(\tau,Y)\} = W(S,Y)$ and $L\{\theta(\tau,Y)\} = V(S,Y)$, these equations assume the following solutions

$$W_1(S,Y) = C_1 e^{\sqrt{S}Y} + C_2\, e^{-\sqrt{S}Y} - \frac{C_3}{(\Pr-1)S} e^{M_1 Y} - \frac{C_4}{(\Pr-1)S} e^{-M_1 Y} \tag{4}$$

$$V_1(S,Y) = C_3 e^{M_1 Y} + C_4\, e^{-M_1 Y} \tag{5}$$

$$W_2(S,Y) = C_5 e^{\sqrt{A}Y} + C_6\, e^{-\sqrt{A}Y} - \frac{C_7}{\mu_R(\Pr.S/\alpha_R - A)} e^{M_2 Y} - \frac{C_8}{\mu_R(\Pr.S/\alpha_R - A)} e^{-M_2 Y} \tag{6}$$

$$V_2(S,Y) = C_7 e^{M_2 Y} + C_8\, e^{-M_2 Y} \tag{7}$$

where $M_1 = \sqrt{\Pr S}$, $\quad M_2 = \sqrt{\dfrac{\Pr S}{\alpha_R}}$, $\quad A = \left(\dfrac{C_a}{\mu_R} S + \dfrac{1}{(\mu_R\, Da)}\right)$

Also, the Laplace transformation of the boundary conditions, yields:

$$W_1(S,0) = 0.0, \quad V_1(S,0) = \frac{1}{S}, \; W_2(S,1) = 0.0, \quad V_2(S,1) = \frac{1}{S}\; W_1(S,r) = W_2(S,r),$$

$$V_1(S,r) = V_2(S,r), \; \frac{\partial W_1}{\partial Y}(S,r) = \mu_R \frac{\partial W_2}{\partial Y}(S,r) = 0.0, \; \frac{\partial V_1}{\partial Y}(S,r) = K_R \frac{\partial V_2}{\partial Y}(S,r) = 0.0$$

The constant C_1 to C_8 are found after inserting Eqs. (4-7) into the boundary conditions. Equations (4-7) are inverted using a computer program based on the Riemann-sum approximation.

Results and discussion

Figure 2 shows the spatial temperature distribution at different thermal diffusivity ratios α_R. Here, the porous domain is in direct contact with the heated wall. Porous domains of higher thermal diffusivity produce higher α_R ratios. In this situation the porous layer diffuses more heat as its diffusivity increases and this leads to an increase in both domain temperatures. This is traced from another point of view by plotting the transient temperature distribution as shown in Fig. 3. Figure 4 shows the spatial velocity distribution at different thermal diffusivity ratios. Due to its additive microscopic frictional drag term (Darcy term), the porous domain has a much lower velocity as compared to the clear domain velocity. Porous domains with larger thermal diffusivity (or high α_R) diffuse more heat from the wall to both domains and this in turn increases the buoyancy effect, which is the driving force for the flow. This leads to an increase in the velocity. Figure 5 shows the spatial temperature distribution at different thermal conductivity ratios K_R. Here the thermal conductivity ratio K_R may be increased by decreasing the clear domain thermal conductivity. This in turns leads to a reduction in the heat carried from the heated wall to both domains and as a result, lower temperatures are attained in this situation.

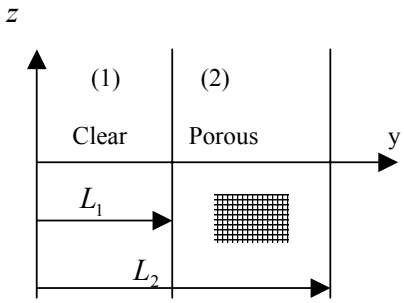

Figure 1: Schematic diagram of the problem under consideration.

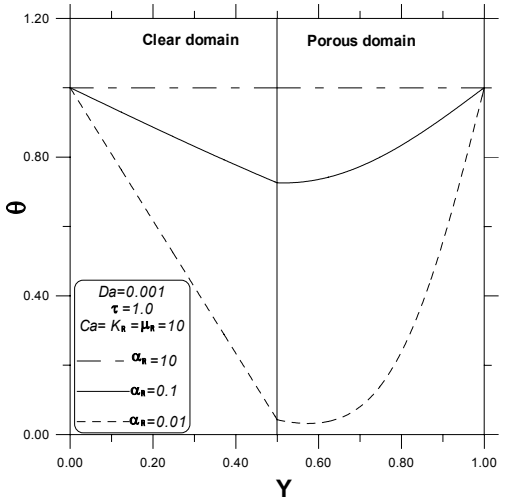

Figure 2: Spatial temperature distribution at different thermal diffusivity ratios.

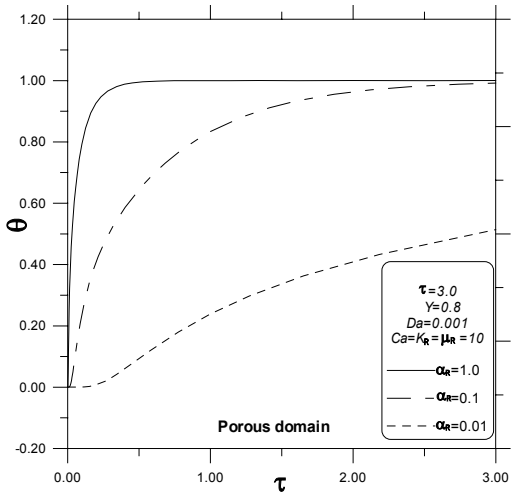

Figure 3: Transient temperature distribution at different thermal diffusivity ratios

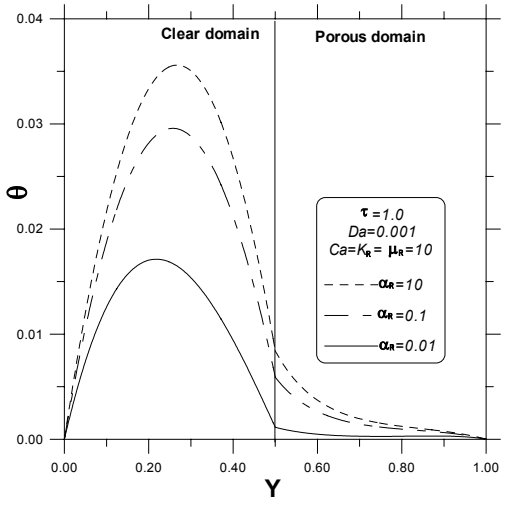

Figure(): Spatial velocity distribution at different thermal diffusivity ratios.

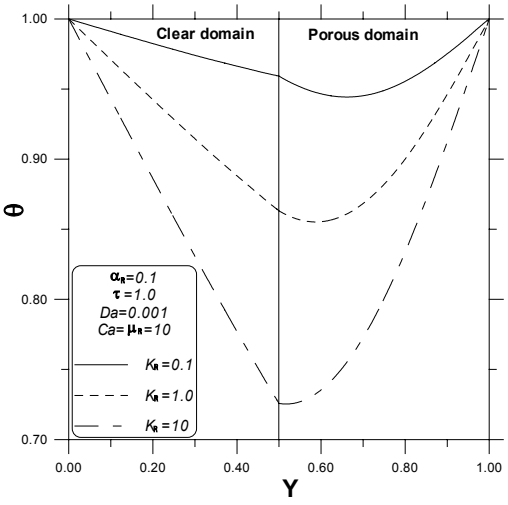

Figure(): Spatial temperature distribution at different thermal conductivity ratios.